

A Robust UAV-Based Approach for Power-Modulated Jammer Localization Using DoA

Zexin Fang*, Bin Han*, and Hans D. Schotten*[†]

*University of Kaiserslautern (RPTU), Germany

[†]German Research Center for Artificial Intelligence (DFKI), Germany

Abstract—Unmanned aerial vehicles (UAVs) are well-suited to localize jammers, particularly when jammers are at non-terrestrial locations, where conventional detection methods face challenges. In this work we propose a novel localization method, sample pruning gradient descend (SPGD), which offers robust performance against multiple power-modulated jammers with low computational complexity.

Index Terms—UAV; direction of arrival (DoA); jamming attack; power-modulation

I. INTRODUCTION

In recent years, unmanned aerial vehicles (UAVs), especially low-altitude UAVs, are becoming a popular solution for reliable wireless communication in a variety of applications [1]. Compared to current terrestrial base stations, UAV-mounted base stations can surpass terrain-related signal propagation issues, while also offering solutions for unexpected and temporary communication demands [2]. Conversely, UAV-mounted jamming attacks can be more effective against terrestrial communication systems compared to terrestrial jammers [3]. Considering that a hovering UAV is easily noticeable, a sophisticated attacker may place UAV-mounted jammers or drop jammers with UAV discreetly in inconspicuous locations, such as bird nests or building rooftops. Additionally, those jammers can also be in disguise to blend in with the environment, making them harder to spot. Given the potential risk outlined above, it is crucial to locate jammers in a three dimensional (3D) space. Assuming the jammer is omni-directional, passive jammer localization methods such as packet delivery ratio (PDR) [4], weighted centroid localization (WCL) [5], and adaptive least-squares (ASL) method [6] can be used for jammer localization. However, those methods commonly require a massive number of affected network nodes and cannot provide altitude estimation.

In the scope of high-accuracy 3D source localization in wireless networks, joint received signal strength (RSS) or direction of arrival (DoA) measurements can be used to localize source with linear estimator [7]. Hybrid RSS and DoA measurements can also be used to precisely estimate source localization with semi-definite programming (SDP) algorithms [8]. In the mean time, UAVs are also considered well-suited for DoA measurements because they can operate with minimal Non-Line-of-Sight (NLOS) interference. This feature ensures high-accuracy DoA estimation, enabling precise source localization with UAVs [9].

Practically, the transmitting power and antenna patterns of jamming sources are usually unknown. In some scenarios, jammers can be even power-modulated, constantly altering their transmission power. In this case, localization methods based on RSS can be unreliable, as evidenced in [10], due to their dependency on the a constant transmission power to estimate the distance. On the other hand, DoA-based localization does not require the transmission power to be constant. Instead, their accuracy is linked with jamming to signal ratio (JSR), as revealed in [11]. This suggests that DoA-based localization tends to be more resilient than RSS-based localization, when transmission power and antenna patterns are unknown.

Most studies on DoA localization assume a fixed normal distribution for the estimation error, reveals a gap in accounting for the variability and complexity of real-world jammer behaviors and radio environment. In this work, we consider directional jammer antenna patterns and DoA measurement errors dependent on the JSR. Unlike prior research, we acknowledge the uncertainty of DoA resolution in UAV-based jammer localization due to power modulation of jammers. To address this, we propose sample pruning gradient descend (SPGD) for robust localization in such scenarios. The remainder of this paper is structured as follows: In Sec. II, we introduce the propagation model and discuss DoA estimation error. Sec. III presents localization techniques using DoA, while Sec. IV validates these techniques through numerical simulations. Sec. V concludes this work.

II. PRELIMINARY

A. Propagation model

Jamming signals attenuate as they travel through the air, influenced by environmental factors like obstacles, terrain, and weather conditions. As a result, the received jamming power can be modeled by a log-normal path loss model [10]:

$$P_j(d) = P_j(d_0) - 10n_p \log\left(\frac{d}{d_0}\right) + X_\sigma, \quad (1)$$

$$X_\sigma \sim \mathcal{N}(0, \sigma), \quad (2)$$

where $P_j(d)$ represents the received jamming signal power at distance d , and $P_j(d_0)$ denotes the jamming power at the reference distance d_0 . n_p signifies the path loss factors. Additionally, X_σ is a log-normal random variable with a mean

and standard deviation, thereby modeling the environmental factors. The JSR can then be defined as,

$$\text{JSR} = P_j(d_j) - P_s(d_s), \quad (3)$$

where d_j represents the distance from the jammer to the receiver, and d_s indicates the distance from the signal source to the receiver.

B. DoA estimation model

DoA estimation is a well-established field with various techniques, including multiple signal classification (MUSIC), estimation of signal parameters via rotational invariance technique (ESPRIT), and fast orthogonal search (FOS) [12], [13], [14]. DoA estimation involve two parameters: elevation and azimuth. Elevation refers to the angle in the vertical plane, measuring the height relative to the horizontal plane. Azimuth, on the other hand, is the angle in the horizontal plane.

Considering $P_j \gg P_s$ in jamming affected area, the signal can be seen as interference to jamming DoA estimation. In [11], it is shown that the Cramer-Rao bound (CRB) is associated with the JSR. The finding also indicated that the performance of any non-ideal DoA estimator will converge above the CRB, depicted in Fig. 1. Thus, the noisy DoA estimation $[\theta_n^\circ, \phi_n^\circ]^T$ can be modelled as,

$$\theta_n^\circ = \theta_n + e_d, \quad (4)$$

$$\phi_n^\circ = \phi_n + e_d, \quad (5)$$

$$e_d \sim \mathcal{N}\left(0, \frac{\sqrt{\sigma_d}}{2}\right), \quad (6)$$

where $\theta_n \in (-\pi, \pi)$ and $\phi_n \in (-\frac{\pi}{2}, \frac{\pi}{2})$ are the true value of azimuth and elevation, respectively; σ_d indicates the error power of DoA.

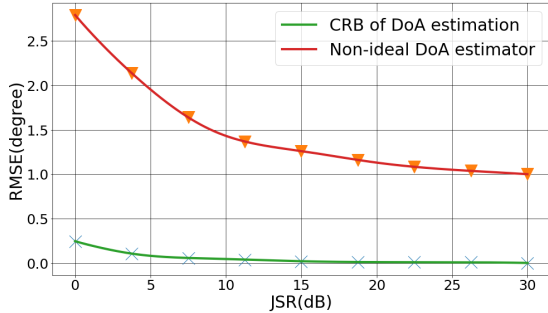


Fig. 1: CRB of DoA estimation and non-ideal DoA estimator

III. METHODOLOGY

A. Jammer localization via least squared estimation (LSE)

The jammer localization problem can be formulated as an optimization problem, which can be solved with LSE. This optimization problem has been formulated [15],

$$\hat{\mathbf{p}} = \underset{\mathbf{p}}{\operatorname{argmin}} \sum_{n=1}^N \left\{ (\mathbf{o}_{1n}^T (\mathbf{p} - \mathbf{p}_n^\circ))^2 + (\mathbf{o}_{2n}^T (\mathbf{p} - \mathbf{p}_n^\circ))^2 \right\} \quad (7)$$

where \mathbf{o}_{1n} and \mathbf{o}_{2n} are the orthogonal vectors, with

$$\mathbf{o}_{1n} = [-\sin \theta_n, \cos \theta_n, 0]^T, \quad (8)$$

$$\mathbf{o}_{2n} = [\cos \theta_n \sin \phi_n, \sin \theta_n \sin \phi_n, -\cos \phi_n]^T. \quad (9)$$

Meanwhile, \mathbf{p}_n° indicates position of UAV with estimation error, considering $\mathbf{p}_n^\circ = [x_n + e_p, y_n + e_p, z_n + e_p]^T$ and $e_p \sim \mathcal{N}\left(0, \frac{\sqrt{\sigma_p}}{3}\right)$. Similarly, σ_p is position error power.

The closed-form solution of Eq.(7) can be obtained,

$$\hat{\mathbf{p}} = (\mathbf{A}^T \mathbf{A})^{-1} \mathbf{A}^T \mathbf{b}, \quad (10)$$

where

$$\mathbf{A} = \begin{bmatrix} \mathbf{o}_{11}^T \\ \vdots \\ \mathbf{o}_{1N}^T \\ \mathbf{o}_{21}^T \\ \vdots \\ \mathbf{o}_{2N}^T \end{bmatrix}; \mathbf{b} = \begin{bmatrix} \mathbf{o}_{11}^T \mathbf{p}_1^\circ \\ \vdots \\ \mathbf{o}_{1N}^T \mathbf{p}_N^\circ \\ \mathbf{o}_{21}^T \mathbf{p}_1^\circ \\ \vdots \\ \mathbf{o}_{2N}^T \mathbf{p}_N^\circ \end{bmatrix}.$$

In many cases, the performance of LSE can be further improved by incorporating a weight matrix to differentiate estimations. In [15], a weight matrix is constructed with respect to the distance to the source with $w_n = 1 - \frac{d_n}{\sum_{n=1}^N d_n}$. However, in our scenario where the antenna pattern and transmitting power of the jamming source are unknown, modeling the weight with the distance to the source is not feasible. Alternatively, considering that the measurement error is linked with JSR, it can be utilized to construct a weight matrix. For $\mathbf{J} = [\text{JSR}_1, \dots, \text{JSR}_n, \text{JSR}_1, \dots, \text{JSR}_n]^T$, a weight matrix can be formulated,

$$\mathbf{W} = \frac{2 \times 10^{\frac{\mathbf{J}}{2n_p}}}{\sum(\mathbf{J})}. \quad (11)$$

Then, the closed-form solution of weighted least squared estimation (WLSE) can be written,

$$\hat{\mathbf{p}} = (\mathbf{A}^T \mathbf{W} \mathbf{A})^{-1} \mathbf{A}^T \mathbf{W} \mathbf{b}. \quad (12)$$

As many of previously mentioned studies have shown, LSE and WLSE can achieve a localization accuracy within a few meters when σ_d is several degrees. While more precise techniques like maximum likelihood estimation (MLE) exist, they typically require much higher computational resources. Considering that jammer localization within several meters is sufficient, LSE and WLSE offer a practical balance between precision and efficiency.

B. SPGD method

The Gradient descend (GD) algorithm is commonly used to solve localization problems [16]. It is highly valued for its adaptability and computational efficiency. The optimization problem can be rewritten as minimizing the gradient vectors (depicted in Fig. 2),

$$\hat{\mathbf{p}} = \underset{\mathbf{p}}{\operatorname{argmin}} \sum_{n=1}^N \mathbf{g}_n, \quad (13)$$

$$\mathbf{g}_n = -(\mathbf{p} - \mathbf{p}_n^\circ + \mathbf{u}_n \times \|\mathbf{p} - \mathbf{p}_n^\circ\|), \quad (14)$$

where \mathbf{u}_n is the unit vector from the true position \mathbf{p}_{tr} .

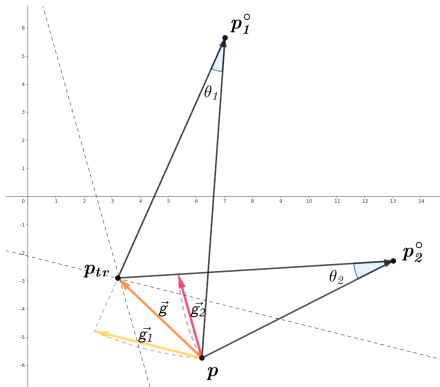


Fig. 2: Gradient vectors of DoAs

$$\mathbf{u}_n = \left[\frac{1}{\sec \theta_n^\circ \sec \phi_n^\circ}, \frac{\sin \theta_n^\circ}{\sec \phi_n^\circ}, \sin \phi_n^\circ \right]^T. \quad (15)$$

To ensure robust estimation while reducing computational complexity, we propose the SPGD method. At each iteration, a proportion of samples with the largest errors relative to the current estimation are discarded. The detailed algorithm is outlined in Algorithm 1.

Algorithm 1: SPGD

```

1 Input: A set contains all coordinate  $\mathcal{P}$ ; a set contains all unit vectors  $\mathcal{U}$ ;
   learning rate and learning decay factor  $\alpha$  and  $\beta$ ; sample pruning rate  $\eta$ ;
   iteration number  $K$ 
2 Output: estimated coordinate  $\mathbf{p}$ .
3 Function SPGD :
4   get  $\mathcal{P}$  and  $\mathcal{U}$ ;
5   initialize  $\mathbf{p} = \frac{1}{N} \sum_{n=1}^N \mathbf{p}_n^\circ$ ;
6   for  $k = 1 : K$  do
7      $\mathbf{g} = \sum_{n=1}^N \mathbf{g}_n$ ;
8      $\mathbf{p} = \mathbf{p} + \alpha \times \mathbf{g}$ ;
9      $\alpha = \alpha \times \beta$ ; //reduce learning rate
10     $\mathcal{D} \leftarrow \{d_n = \|\frac{\mathbf{p} - \mathbf{p}_n^\circ}{\|\mathbf{p} - \mathbf{p}_n^\circ\|} - \mathbf{u}_n; 1 \leq n \leq N\}$ ;
        //errors to current estimation
11     $n_r = \max(N \times \eta, 1)$ ;
12     $\mathcal{N}_r \leftarrow \{j = \text{argmax}_{n \leq n_r} d_n\}$ ; //select samples with largest errors
13    if  $N - n_r \geq 3$  then
14      for  $j \in \mathcal{N}_r$  do
15        remove  $j_{\text{th}}$  elements from  $\mathcal{P}, \mathcal{U}$ 
16      end
17    end
18     $N = N - n_r$ 
19  end
20  Output  $\mathbf{p}$ 
21 end

```

IV. EVALUATION OF METHODOLOGY

A. Jammer antenna pattern

In this work, we model the jammer's antenna pattern as directional, utilizing a helical antenna. Its main lobe is oriented towards $\theta = \pi$, as depicted in Fig. 3. The helical antenna exhibits a dynamic range of 20dB.

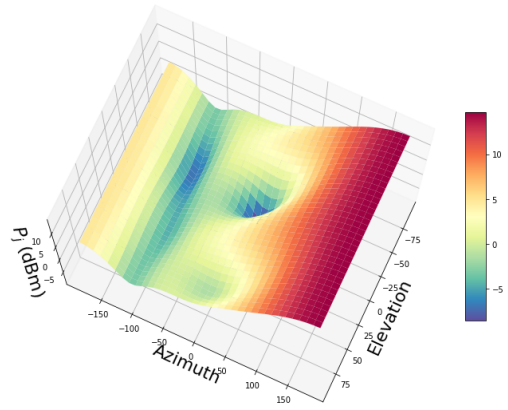


Fig. 3: Antenna pattern of helical antenna

B. Jammer Localization in an ideal scenario

To assess the localization performance of the aforementioned techniques, we consider an ideal scenario where the UAV cruises within a large area. The jammer A is positioned at the center with a certain level of ambiguity. We assume the signal source is located very far away, with $P_j \gg P_s$.

TABLE I: Simulation setup 1

	Parameter	Value	Remark	
System		$[0 \sim 100, 0 \sim 100, 5 \sim 25]$	Cruising area	
		$[40 \sim 60, 40 \sim 60, 12 \sim 18]$	Jammer location area	
		$\max(P_{tj})$	$5 \sim 25\text{dBm}$	jammer main lobe transmitting power
		P_s	-15dBm	received signal power
		N	8, 20, 40	number of DoAs measurements
		σ_P	3	position error power
SPGD	K	10	Iteration number	
	α	1	learning rate	
	β	0.7	learning decay factor	
	η	0.3	Sample pruning rate	

All simulation results in this paper, including those depicted in Fig. 4 under an ideal scenario, are obtained from 2000 Monte Carlo iterations. WLSE exhibited the best performance across three different number of N , especially when $\max(P_{tj})$ is low. SPGD demonstrated a similar performance to WLSE under 8 estimations are collected. Meanwhile SPGD also shows better performance than LSE while $\max(P_{tj}) = 5$. This indicates a resilience of SPGD to estimation error, especially under limited estimations are collected, where estimation errors are not likely to cancel out. In other cases, LSE outperformed SPGD. However, LSE requires multiple matrix multiplications, leading to computational complexity that is predominantly $\mathcal{O}(2Nq^2)$, where q is the number of sample features, and in this context, $q = 3$. WLSE is more than $\mathcal{O}(2Nq^2)$. Since N is reduced exponentially with SPGD, the computational complexity of SPGD is predominately $\mathcal{O}\left(q \frac{N(1-\eta^K)}{1-\eta}\right)$. In scenarios where $N \gg K$, SPGD demonstrates significantly lower computational complexity compared to LSE. As discussed earlier in Subsec. III-A, SPGD achieves

a balanced trade-off between accuracy and computational complexity.

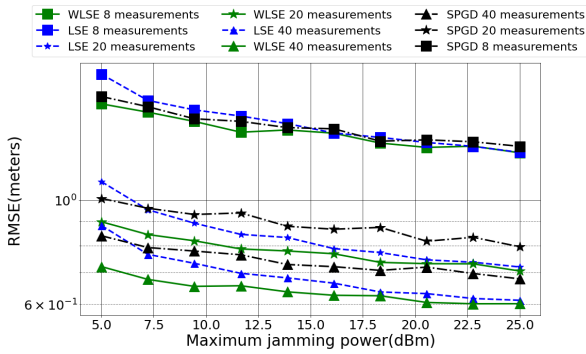


Fig. 4: Antenna pattern of helical antenna

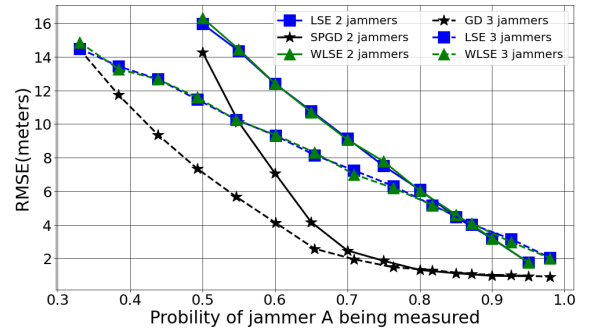
C. Jammer localization in a non-ideal scenario

The presence of power-modulated jammers and other strong signal sources can significantly complicate the localization problem. While many DoA estimation algorithms can resolve multiple DoAs at an increased computational cost, they face significant challenges when dealing with highly coherent signals, such as jamming signals. The author in [11] demonstrated that the DoA of two sinusoidal jamming signals with different frequencies can be resolved when $P_{jA} = P_{jB}$. However, this is only theoretically possible. In practice, due to differences in distance, antenna directionality, and other environmental factors, the condition $|P_{jA} - P_{jB}| \gg 0$ is more likely to hold. In this scenario, accurately resolving the DoA of jamming components other than the largest is unlikely. In contrast to static receiver settings, where the DoAs of multiple sources can be spatially clustered, associating these signal DoAs with the correct sources presents a significant challenge when a cruising UAV serves as the receiver.

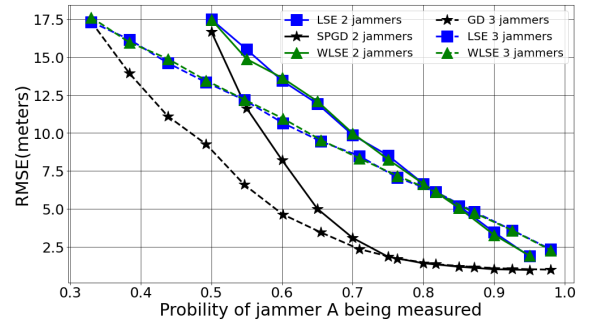
To simplify localization and minimize computational costs, we consider only the DoA of the largest jamming component is solvable, and other components as interference. Assuming M jammers are involved, and given that the cruising center of the UAV is randomly determined with very limited information, the probability of it coinciding with the geometric center is very low. Combining with other random factors, the equal probabilities of estimation $P_A = P_B = \dots = P_M$ can be ignored. Thus, the jammer with the largest probability P can be expected to be localized with minimal efforts. We conduct simulations to localize jammer A with $M = 2, 3$ and $P_A \in [\frac{1}{M}, 1]$, detailed setup follow Tab. I with $N = 40$. The cruising center's lean toward a jammer will also affect localization, so we consider two scenarios: one with a strong lean toward jammer A , and another with a slight lean toward jammer A .

The simulation results are shown in Fig. 5. In both cases, the localization error of SPGD decreased exponentially as P increased, while the errors for WLSE and LSE decreased linearly. SPGD was able to provide much more robust estimations

in complex scenarios by leveraging the correlations among estimations. Meanwhile, a slight degradation in the performance of all localization techniques in *case 2* can be observed. This occurs because DoA measurements from other sources in *case 2* tend to lean more toward a direction orthogonal to that of jammer A , resulting in greater localization errors.



(a) Case 1: strongly leans to jammer A



(b) Case 2: slightly leans to jammer A

Fig. 5: Localization performance under varying P_A

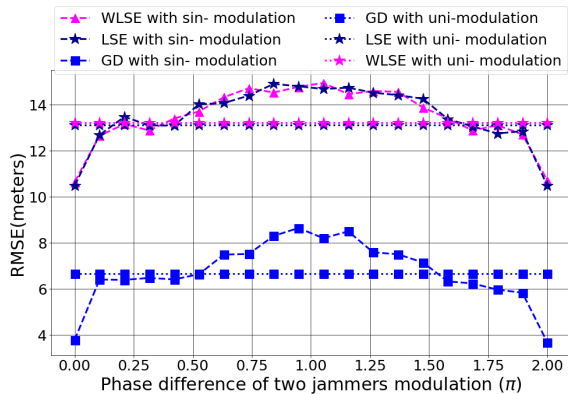
D. Jammer localization under different power-modulation schemes

In this subsection, we delve into the impact of various jammer power-modulation schemes on localization performance. Specifically, we consider the arrangement of two jammers. The jammer was described in Subsec. IV-A, with main lobe transmitting power $\max(P_{tj})$ falling between 5dBm and 25dBm. Initially, we consider two power-modulation schemes:

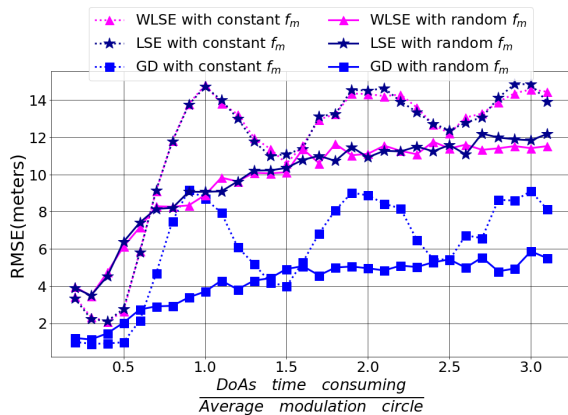
- i) **random uniform modulation:** $\max(P_{tj}^A) \sim \mathcal{U}(5, 20)$;
 $\max(P_{tj}^B) \sim \mathcal{U}(5, 20)$
- ii) **sinusoidal modulation:** $\max(P_{tj}^A) = 12.5 + 7.5 \sin \frac{t}{T}$;
 $\max(P_{tj}^B) = 12.5 + 7.5 \sin (\frac{t}{T} + \Phi)$.

We consider DoA estimations start randomly and the time consuming T_m equals to the modulation circle T . The simulation results are shown in Fig. 6a.

Notably, SPGD outperformed WLSE and LSE across all power-modulation schemes. When the phase difference $\Phi = 0$, it indicates that $\max(P_{tj}^A)$ and $\max(P_{tj}^B)$ vary equally. This uniformity, coupled with the tendency of the randomly determined cruising center to lean towards one jammer, leads to most resolved DoAs being attributed to that jammer. Therefore, at $\Phi = 0$, the impact of **sinusoidal modulation** on



(a) localization errors with regard to modulation phase difference



(b) localization errors in relation to time consuming

Fig. 6: localization errors under different modulation schemes

localization performance is only marginal. At $\Phi = \pi$, the absolute power differences $|\max(P_{tj}^B) - \max(P_{tj}^A)|$ reaches its maximum. Consequently, even if the cruising center lean towards one jammer, the other jammer can still significantly interfere with localization, resulting in large errors.

In **sinusoidal modulation**, the frequency $f_m = \frac{1}{T}$ can either remain constant or exhibit some degree of randomness, represented by $f_m = b\bar{f}_m$ and $b \sim \mathcal{U}(0, 2)$. When $\Phi = \pi$, sinusoidal modulation can significantly affect localization; however, while DoA estimations are done in a short time can mitigate this effect. We demonstrate this relationship with T_m ranging from $0.2T$ to $3.1T$ in Fig. 6b. Constant f_m results in large localization errors, especially when T_m is an integer multiple of T . This occurs because most estimations of first half circle are usually from one jammer, and the second half attributed to another. This pattern also explains localization errors are lower while $T_m = 1.5T, 2.5T$. Once T is accessed, synchronously taken DoA estimations with T can help minimize errors. Conversely, when f_m exhibits randomness, making it inaccessible, its impact is typically reduced compared to a constant f_m .

V. CONCLUSION

In this paper, we have thoroughly investigated the localization of power-modulated jammers using DoA measurements obtained from a UAV. Concerning complex practical scenarios involving multiple jammers and non-ideal DoA resolution, we have proposed a novel SPGD solution for precise localization. It has been demonstrated superior to WLSE and LSE under all power modulation schemes, regarding both robustness and computational complexity.

ACKNOWLEDGMENT

This work is supported partly by the German Federal Ministry of Education and Research within the project Open6GHub (16KISK003K/16KISK004), partly by the European Commission within the Horizon Europe project Hexa-X-II (101095759). B. Han (bin.han@rptu.de) is the corresponding author.

REFERENCES

- [1] J. Tang, G. Chen, and J. P. Coon, "Secrecy Performance Analysis of Wireless Communications in the Presence of UAV Jammer and Randomly Located UAV Eavesdroppers," *IEEE TIFS*, vol. 14, no. 11, pp. 3026–3041, 2019.
- [2] Y. Zhu, G. Zheng, and M. Fitch, "Secrecy Rate Analysis of UAV-Enabled mmWave Networks Using Matérn Hardcore Point Processes," *IEEE JSAC*, vol. 36, no. 7, pp. 1397–1409, 2018.
- [3] Q. Wu, W. Mei, and R. Zhang, "Safeguarding Wireless Network with UAVs: A Physical Layer Security Perspective," *IEEE Wirel. Commun.*, vol. 26, no. 5, pp. 12–18, 2019.
- [4] W. Qipin, W. Xianglin, F. Jianhua *et al.*, "A step further of PDR-based jammer localization through dynamic power adaptation," in *IEEE WiCOM 2015*, 2015, pp. 1–6.
- [5] X. Wei, Q. Wang, T. Wang *et al.*, "Jammer Localization in Multi-Hop Wireless Network: A Comprehensive Survey," *IEEE COMST*, vol. 19, no. 2, pp. 765–799, 2017.
- [6] Z. Liu, H. Liu, W. Xu *et al.*, "Exploiting Jamming-Caused Neighbor Changes for Jammer Localization," *IEEE TPDS*, vol. 23, no. 3, pp. 547–555, 2012.
- [7] A. Heydari and M. Aghabozorgi, "Joint RSSD/AOA Source Localization: Bias Analysis and Asymptotically Efficient Estimator," *Wirel. Pers. Commun.*, vol. 114, pp. 2643–2661, 2020.
- [8] H. Qi, L. Mo, and X. Wu, "SDP Relaxation Methods for RSS/AOA-Based Localization in Sensor Networks," *IEEE Access*, vol. 8, pp. 55 113–55 124, 2020.
- [9] B. Shi, Y. Li, G. Wu *et al.*, "Low-Complexity Three-Dimensional AOA-Cross Geometric Center Localization Methods via Multi-UAV Network," *Drones*, vol. 7, no. 5, 2023.
- [10] P. Tedeschi, G. Oligeri, and R. Di Pietro, "Localization of a power-modulated jammer," *Sensors*, vol. 22, no. 2, 2022.
- [11] A. Osman, M. M. E. Moussa, M. Tamazin *et al.*, "DOA Elevation and Azimuth Angles Estimation of GPS Jamming Signals Using Fast Orthogonal Search," *IEEE TAES*, vol. 56, no. 5, pp. 3812–3821, 2020.
- [12] R. Schmidt, "Multiple emitter location and signal parameter estimation," *IEEE TAP*, vol. 34, no. 3, pp. 276–280, 1986.
- [13] M. J. Korenberg, "Identifying nonlinear difference equation and functional expansion representations: the fast orthogonal algorithm," *Ann. Biomed. Eng.*, vol. 16, pp. 123–142, 1988.
- [14] R. Roy and T. Kailath, "ESPRIT-estimation of signal parameters via rotational invariance techniques," *IEEE TASSP*, vol. 37, no. 7, pp. 984–995, 1989.
- [15] F. Watanabe, "Wireless Sensor Network Localization Using AoA Measurements With Two-Step Error Variance-Weighted Least Squares," *IEEE Access*, vol. 9, pp. 10 820–10 828, 2021.
- [16] Z. Fang, B. Han, and H. D. Schotten, "A Reliable and Resilient Framework for Multi-UAV Mutual Localization," in *IEEE VTC2023-Fall*, 2023, pp. 1–7.